Proceedings of the 20th International Conference on Soil Mechanics and Geotechnical Engineering– Rahman and Jaksa (Eds)

Experimental study to elucidate cementation effect on swelling pressure and montmorillonite basal spacing of bentonite ore

Étude expérimentale pour élucider l'effet de la cimentation sur la pression de gonflement et l'espacement basal de la montmorillonite du minerai de bentonite

Daichi Ito & Hideo Komine
Faculty of Science and Engineering, Waseda University, Tokyo, Japan

ABSTRACT: For the geological disposal of high-level radioactive waste (HLW), the self-sealing capability of bentonite buffer material must be retained for at least several thousand years. However, in the deep ground environment, the occurrence of cementation and the consequent buffer's property changes present important concerns. Few studies have elucidated effects of cementation on self-sealing capability. In this study, swelling properties of the cemented buffer are regarded as similar to natural bentonite ore. A Japanese Na-type bentonite ore is used in experimental works. Undisturbed and reconstituted specimens were prepared to assess their swelling pressure. Results show that the swelling pressure of undisturbed specimens is about half of reconstituted specimens. Also, X-ray diffraction is used for specimens before and after swelling pressure tests for comparison of montmorillonite basal spacing. Results show fewer water molecules in the interlayer of montmorillonite in undisturbed specimens with the same water content. Infiltration of water molecules to the interlayer of montmorillonite might be inhibited by cementation in the undisturbed specimens. The swelling pressure was reduced compared to that of reconstituted specimens.

RÉSUMÉ : Pour le stockage géologique des déchets hautement radioactifs (HLW), la capacité d'auto-étanchéité du matériau tampon de bentonite doit être conservée pendant au moins plusieurs milliers d'années. Cependant, dans l'environnement profond, la cimentation et les modifications de propriété de la zone tampon qui en résultent posent des problèmes importants. Peu d'études ont élucidé les effets de la cimentation sur la capacité d'auto-obturation. Dans cette étude, les propriétés de gonflement du tampon cimenté sont considérées comme similaires à celles du minerai de bentonite naturel. Un minerai de bentonite de type Na japonais est utilisé dans les travaux expérimentaux. Des échantillons non perturbés et reconstitués ont été préparés pour évaluer leur pression de gonflement. Les résultats montrent que la pression de gonflement des échantillons non perturbés est d'environ la moitié des échantillons reconstitués. En outre, la diffraction des rayons X est utilisée pour les échantillons avant et après les tests de pression de gonflement pour la comparaison de l'espacement basal de la montmorillonite. Les résultats montrent moins de molécules d'eau dans l'intercalaire de montmorillonite dans les spécimens non perturbés avec la même teneur en eau. L'infiltration des molécules d'eau dans la couche intermédiaire de montmorillonite pourrait être inhibée par la cémentation dans les échantillons non perturbés. La pression de gonflement a été réduite par rapport à celle des échantillons reconstitués.

KEYWORDS: Bentonite, Cementation, Swelling, X-ray diffraction

1 INTRODUCTION

For the geological disposal of HLW, bentonite-based buffer materials must have low permeability and self-sealing properties, which means that the buffer material seals the surrounding gaps through swelling deformation for thousands of years (Ogata et al. 1999). Figure 1 is conceptual figure of geological disposal (JAEA 2017). Because the buffer material would be placed in conditions such as high groundwater pressure, temperatures, and unusual water chemistry, it is possible for them to solidify because of long-term cementation and changes in physical properties, such as swelling. However, reproducing and evaluating long-term and complicated phenomena such as cementation are difficult to achieve solely through laboratory experiments. Past studies have confirmed the stability of montmorillonite minerals (Pusch 1983). Consolidation and strength properties have been evaluated (Towhata et al. 1998) using bentonite ore existing deep underground and using natural analogue concepts (Alexander et al. 2015). The authors thought it possible to evaluate age changes of cementation, such as swelling, on the physical properties of buffer.

For this study, undisturbed specimens that retained the cementation of ore and reconstituted specimens from which cementation had been physically removed were prepared. Swelling pressure on these specimens was measured under volume change suppression to evaluate the cementation effects on the swelling pressure. Furthermore, X-ray diffraction (XRD) was performed for specimens before and after swelling pressure measurements for revealing mechanisms of declining swelling pressure in undisturbed specimens from the viewpoint of montmorillonite basal spacing.

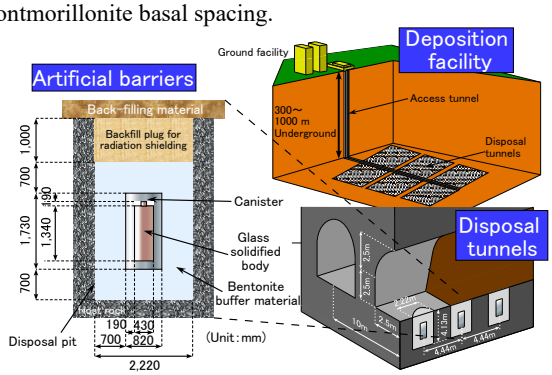

Figure 1. Conceptual figure of geological disposal facility

Figure 2. Appearance of bentonite ore used for this study

2 MATERIALS AND SPECIMEN PRODUCTION

2.1 *Fundamental characteristics of bentonite ore*

Na-type bentonite ore mined from the Tsukinuno mine in Japan was used for this study. The main product from the Tsukinuno mine, Kunigel V1 (Kunimine Co., Ltd.), is a candidate material for buffer and backfill materials in Japanese HLW disposal. Based on earlier geological studies (Ito et al. 1999; Sawada 1996), the geological age is estimated as about 10 million years ago. It was generated by diagenesis. Figure 2 portrays the ore appearance. Table 1 presents the ore characteristics.

For measuring various properties, the ore was dried in a drying oven set at 110℃ for one day. Then it was crushed to a particle size of 0.425 mm or less (hereinafter, approx. 0.425 mm) as described in an earlier report (Ito et al. 2006). The soil particle density, liquid limit, and plastic limit were measured using a method reported earlier in the relevant literature (Komine & Ogata 1991). Cation exchange capacity (CEC) and ion concentration adsorbed in the montmorillonite interlayer were measured using the Japanese Geotechnical Society standard (JGS 2009). The montmorillonite content was calculated from results of methylene blue (MB) adsorption tests (JIS 2019), assuming that the adsorption amount of the pure montmorillonite sample was 140 mmol / 100 g. From XRD test, the ore was found to contain quartz, plagioclase, calcite, and biotite asides from montmorillonite.

Table 1. Fundamental characteristics of the ore

Properties	*Value*	*Unit*
Soil particle density	2.77	Mg/m^3
Liquid limit	419.1	%
Plastic limit	29.2	%
Plasticity index	389.9	-
Montmorillonite content	44.7	%
Swell index	12	mL/2g
CEC	39.3	cmol (+)/kg
Ion concentration (Na^+)	42.5	cmol (+)/kg
Ion concentration (Ca^{2+})	10.2	cmol (+)/kg
Ion concentration (Mg^{2+})	0.8	cmol (+)/kg
Ion concentration (K^+)	Lower than determination limit (0.8)	cmol (+)/kg

2.2 *Method of producing specimens*

To evaluate cementation effects on swelling pressure, both undisturbed specimens retaining cementation of the ore and reconstituted specimens with physically removed cementation were prepared and used for experiments. The undisturbed specimens were formed into a cylindrical shape with 28 mm diameter and 10 mm height with trimming tools such as a cutter ring, knife, and trimmer. The reconstituted specimens were made by powdering ore samples that had been crushed to a particle size of approx. 0.425 mm. The particle size was adjusted to 0.850-2 mm using a crusher and sieves and then compacting the crushed samples by application of a static load. The water contents of undisturbed specimens at the start of the test were 9.4 to 13.9%. The water contents of the reconstituted specimens with particle size of approx. 0.425 mm were 6.1 to 10.8%. The particle sizes of 0.850-2 mm were 11.2-12.5%.

3 SWELLING PRESSURES IN UNDISTURBED AND RECONSTITUTED SPECIMENS

Experiments of swelling pressure measurements were conducted using the test device depicted in Figure 3 (Komine et al. 2009). With this experimental device, distilled water was supplied from the lower part of the specimen. Swelling deformation of the specimens was restrained using a SUS316L ring on the horizontal direction and by tightening the clamp knob in the vertical direction. In this experiment, the time course of swelling pressure, and the relation between maximum value of swelling pressure during the test (hereinafter designated as the maximum swelling pressure) and the drying density of the specimen were investigated.

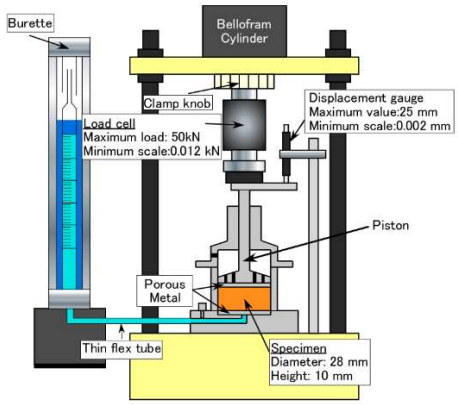

Figure 3. Swelling pressure measurement device

Figure 4-6 shows the time course of swelling pressure of the undisturbed specimens and the reconstituted specimens (particle size: approx. 0.425 mm, 0.850-2 mm), respectively. In the reconstituted specimens, swelling pressure increased sharply immediately after the start of the test for both approx. 0.425 mm and 0.850-2 mm. It then became constant after about 5000 min. However, in the undisturbed specimens, the increase in swelling pressure was slower than in the reconstituted specimens. In fact, it took more than 15,000 minutes for all specimens to reach constant swelling pressure. Presumably, the soil particle structure of the undisturbed specimen is complicated by cementation effects. For that reason, it takes a longer time for the swelling pressure development accompanying water absorption. Additionally, regarding the degree of specimen saturation after the test, the reconstituted specimens (approx. 0.425 mm particle size) were 97.7-105.0%; the reconstituted specimens (0.850-2 mm particle size) were 97.3-107.0%. The undisturbed specimens were 94.3-113.8%. Since all the values were close to 100%, it can be considered that all the specimens are saturated at the end of the test.

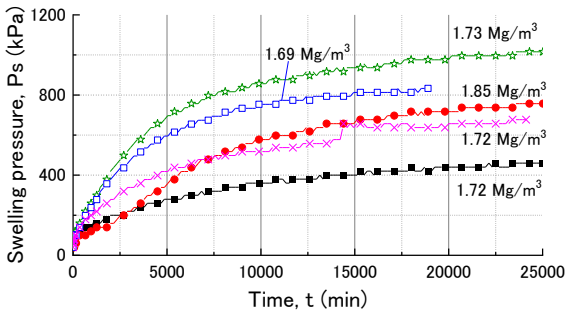

Figure 4. Time course of swelling pressure (Undisturbed specimens)

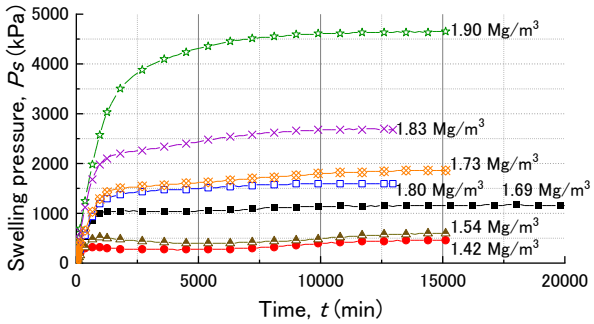

Figure 5. Time course of swelling pressure (Reconstituted specimens, approx. 0.425 mm particle)

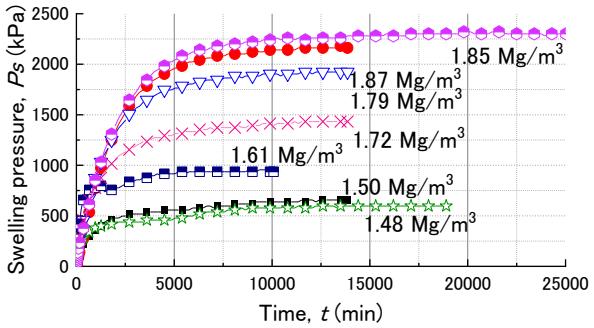

Figure 6. Time course of swelling pressure (Undisturbed specimens, 0.850~2 mm particle)

Figure 7 shows the relation between maximum swelling pressure and the dry density of undisturbed specimens and reconstituted specimens. In the reconstituted specimens, the maximum swelling pressure tends to increase as the dry density increases, irrespective of the particle size. Furthermore, no significant difference was found in maximum swelling pressure in the 1.4-1.7 Mg/m^3 range, but the difference gets spreading at dry densities higher than 1.8 Mg/m^3. When the dry density is high, the voids in the initial state are small. Probably for that reason, swelling deformation of the particles by water absorption does occur. Therefore, the cementation effects of particles might be remaining. Although the values of the undisturbed specimens vary widely, the maximum swelling pressure tended to be smaller in all specimens than in the reconstituted specimens. From these experimentally obtained results, the undisturbed specimen has a longer convergence time to reach the maximum swelling pressure because of cementation. The maximum swelling pressure declines to about half that of the reconstituted specimen with the same dry density.

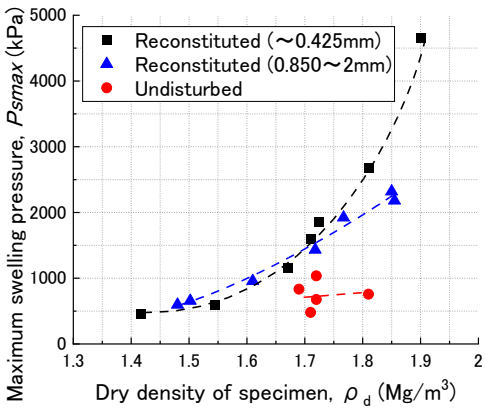

Figure 7. Relation between maximum swelling pressure and the specimen dry density

4 MONTMORILLONITE BASAL SPACING OBSERVATION BY X-RAY DIFFRACTION BEFORE AND AFTER SWELLING PRESSURE MEASUREMENTS

4.1 *Testing device and procedures*

To clarify reasons why the maximum swelling pressure of the undisturbed specimens remains lower than that of the reconstituted specimens, XRD was applied to specimens before and after the swelling pressure test (s.p. test) to measure the basal spacing of montmorillonite crystals d_{001}. Earlier studies showed that the montmorillonite basal spacing and the number of water molecules existing between the layers are related, as shown in Figure 8 (Wang et al. 2020; Morodome & Kawamura 2009; Ferrage et al. 2005; Sato et al. 1992; Watanabe & Sato 1988). From this figure, as the number of water molecules existing between layers increases, basal spacing d_{001} increases gradually. Furthermore, the basal spacing is calculable from the peak position of montmorillonite by Bragg's law in Eq. 1.

$$d_{001} = n\lambda/2 \sin\theta_{peak} \quad (1)$$

Therein, λ represents the incident wave wavelength (=1.5418Å for Cu Kα), n is a positive integer (=1), and θ_{peak} is θ at peak maximum.

For this investigation, the device shown in Figure 9 was used to measure the swelling pressure. An important feature of this experimental device is that the mold consists of multiple rings for performing XRD measurements. During the experiment, water was supplied from the lower part of the specimen. Regarding the water absorption and swelling of the specimen, the SUS303 ring (28 mm inner diameter, 5 mm thickness, 2 mm height) was tightened on the horizontal side. The screw on the lower part of the device was fettered in the vertical pressure of 250-300 kPa. The lower surface of the specimen and the bottom plate were surely brought into mutual contact. The upper part of the device was also restrained by tightening four screws.

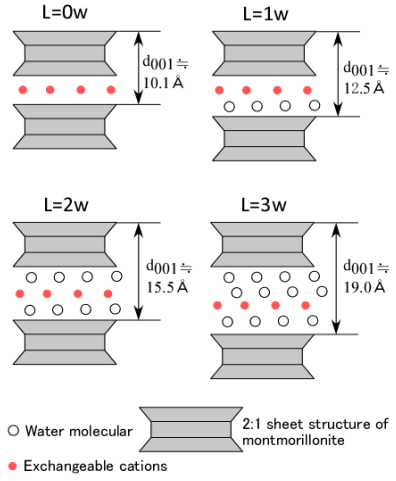

Figure 8. Relation between the number of water molecules present and the montmorillonite basal spacing

The procedure and operation of XRD observation before and after the s.p. test was referred from a report of an earlier study (Wang et al. 2020). First, 2-3 SUS303 rings with 2 mm thickness were stacked. Two-sheet set rings with 0.30 mm thickness were sandwiched between the rings to form a mold as shown in Figure 10. The undisturbed specimens and reconstituted specimens (approx. 0.425 mm particle size) were made using the method described in 2 and were installed into the mold. Next, the basal

spacing d_{001} of montmorillonite in the specimens was observed using XRD under the measurement conditions presented in Table 2. An X-ray diffractometer (RINT-Ultima III; Rigaku Corp.) was used for XRD observation. After XRD observation, the swelling pressure experiment device was assembled. Then the supply of distilled water and the s.p. test were started simultaneously. After measuring the swelling pressure for a predetermined period, the test device was disassembled. Then both the specimen and mold were removed. The two-sheet set rings were taken out first. Then the specimen was cut into 2 mm thick pieces using a jigsaw with 0.20-0.25 mm blade thickness. After cutting, the specimens were sealed with paraffin film to prevent evaporation of water until XRD observation. Then, d_{001} was observed under the conditions shown in Table 2. After observation, the water contents of the specimens were measured. Table 3 presents the implementation cases of the experiment.

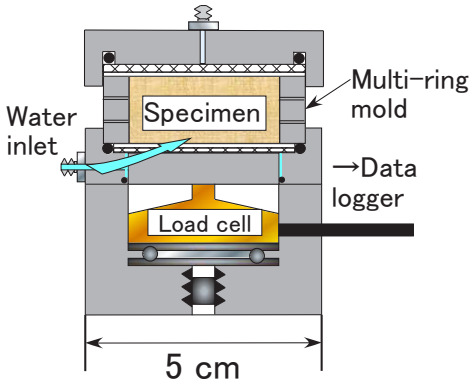

Figure 9. Swelling pressure device with multi-ring mold

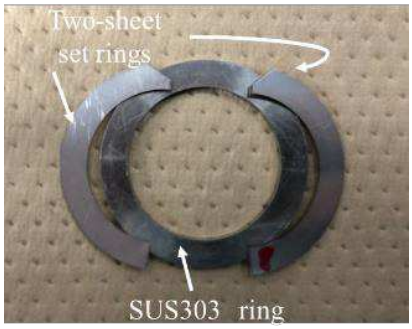

Figure 10. Configuration of multi-ring mold

Table 2. Measurement condition of XRD

Optical system	Focal geometry
Incident wave source	CuKα
Measurement range	2.7 ~ 20°
Scanning step	0.02°
Scanning speed	10°/min
Divergence slit	1/8°
Scattering slit	8.00 mm
Light-receiving slit	13.00 mm

4.2 *Comparison of montmorillonite basal spacing between undisturbed specimens and reconstituted specimens and consideration of difference in swelling pressure*

Figure 11 shows the relation between the maximum swelli ng pressure and the specimen dry density. This figure sho ws that the maximum swelling pressure of the undisturbed specimens tended to remain lower than that of the reconstituted specimens, as in the experimentally obtained results in 3. Although the experimental device differs from the experiment in 3, the measured values of the swelling pressure of the undisturbed specimens are almost identical to the 750-1000 kPa of 1.7-1.8 Mg/m^3. Therefore, the effect of the equipment difference on the swelling pressure value is expected to be negligible.

Table 3. Implementation cases of the experiment

	Specimen dry density (Mg/m^3)	Specimen Height (mm)	Test period (day)	XRD observation with s.p. test
Undisturbed specimens	1.79	4	5	Only after
	1.74	6	2	Only after
	1.75	4	5	Before and after
	1.72	4	6	Before and after
Reconstituted specimens	1.77	4	5	Only after
	1.77	6	2	Only after
	1.84	4	5	Before and after

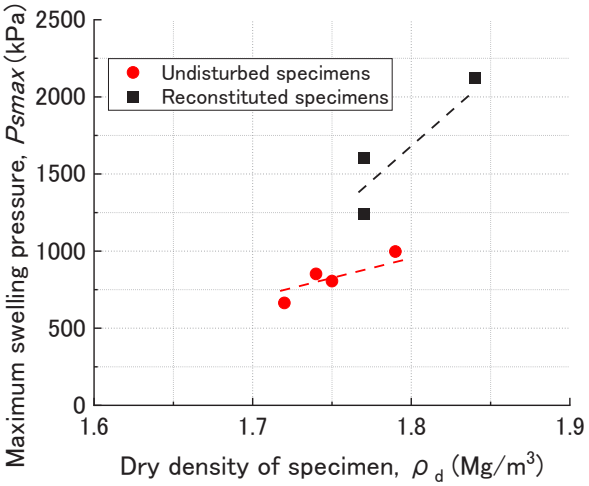

Figure 11. Relation between maximum swelling pressure and specimen dry density

Figure 12 and Figure 13 respectively show examples of XRD observation results before and after the s.p. test of undisturbed specimens and reconstituted specimens. In the undisturbed specimens, the montmorillonite peak before the s. p. test (water content w = 11.9%) is located at 5.8 deg, which is the basal spacing (d_{001} = 15.5 Å) in which two rows of water molecules exist between the montmorillonite layers. Additionally, the peak after the s.p. test is located at 4.7 deg on both the part near the water supply surface (w = 20.2%) and the upper surface (w = 16.1%), which is the basal spacing where three rows of water molecules exist between the layers (d_{001}=19.0 Å). From these, the number of water molecules between montmorillonite layers increased from 2 to 3 rows because of water absorption during the s.p. test in the undisturbed specimens. In the reconstituted

specimens, the peak before the s.p. test (w = 10.7%) exists at 5.8 deg. It is equal to two rows of water molecules between the layers. After the s.p. test, the peak exists 5.8 deg on the water supply surface side (w = 18.1%) and 4.7 deg on the top surface (w = 13.8%). Therefore, the number of water molecules between the montmorillonite layers increased from 2 rows to 3 rows because of water absorption during the s.p. test in the reconstituted specimens.

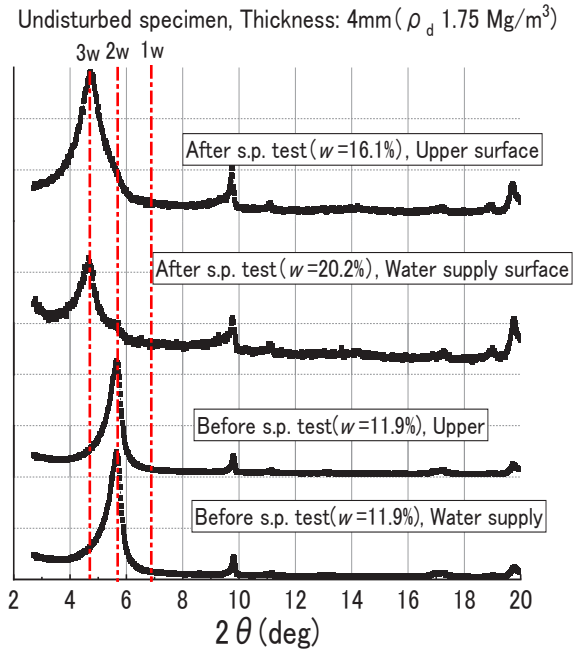

Figure 12. Comparison of XRD observations before and after the s.p. testing of an undisturbed specimen (ρ_d 1.75 Mg/m^3)

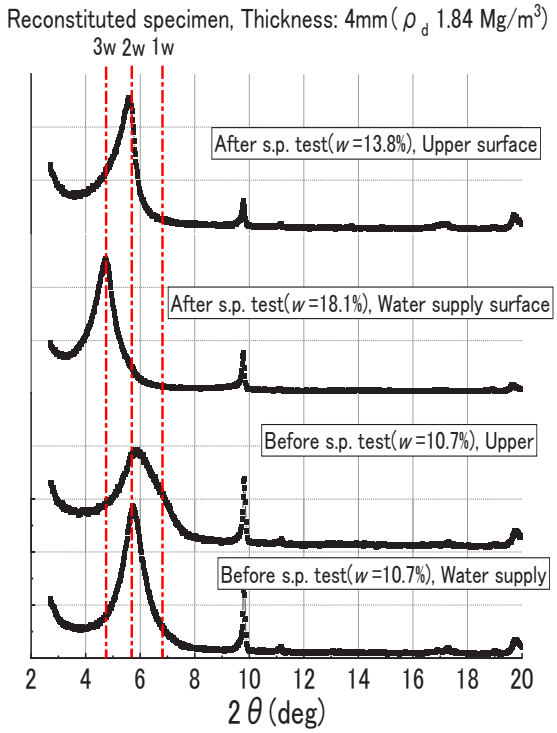

Figure 13. Comparison of XRD observations before and after the s.p. testing of a reconstituted specimen (ρ_d 1.84 Mg/m^3)

Figure 14 portrays the relation between montmorillonite basal spacing d_{001} and the water content of the undisturbed specimens and the reconstituted specimens. From this figure, both the undisturbed specimen and the reconstituted specimen have basal spacing equal to that of two rows of water molecules at w=9-14%, and three rows of water molecules at w=15-20%. The relation between the basal spacing of montmorillonite and the water content is stepwise: it can be characterized as the same tendency as that found in earlier studies (Wang et al. 2020; Morodome & Kawamura 2009). The values of the basal spacing are about the same as those of the undisturbed and reconstituted specimens. Therefore, when particularly addressing only the maximum peak, the cementation effect on the montmorillonite basal spacing d_{001} is only slightly visible.

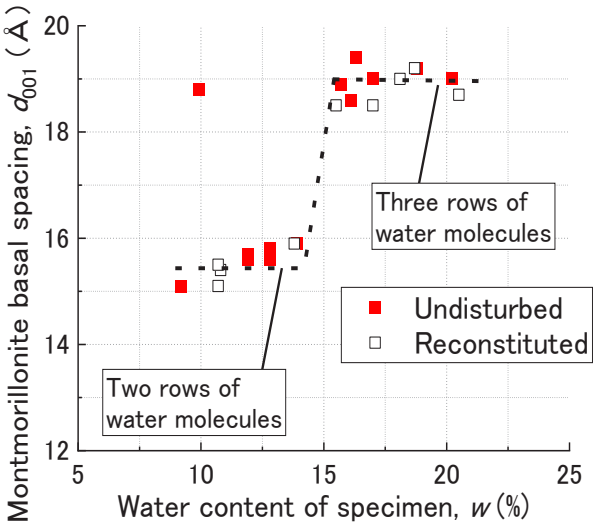

Figure 14. Relation between the montmorillonite basal spacing d_{001} and the water content of specimens

Figure 15 and 16 respectively show the peak shapes of the undisturbed specimen and the reconstituted specimen with water contents of 17.0% and 18.8%. The peak curves shown in these figures are normalized by the maximum peak value for relative comparison. From these figures, in the reconstituted specimens, the basal spacing of three rows of water molecules (2θ=4.7 deg, d_{001}=19.0 Å) is dominant in both water contents. However, in the undisturbed specimens, the peaks for two rows of water molecules (2θ=5.8 deg, d_{001}=19.0 Å) remain at the right shoulder part of the peak of three rows of water molecules, as indicated by arrows in Figures 14 and 15. These results show that the number of water molecules present between the montmorillonite crystal layers in the undisturbed specimens is smaller than that of the reconstituted specimens under the same water content. From these results obtained from the undisturbed specimens, one can infer that the movement and absorption of water molecules between the montmorillonite crystal layers was inhibited by cementation effect. Consequently, the swelling deformation by the intrusion of water between the crystal layers of montmorillonite may be reduced. Presumably, the swelling pressure of undisturbed specimens is lower than that of the reconstructed specimens.

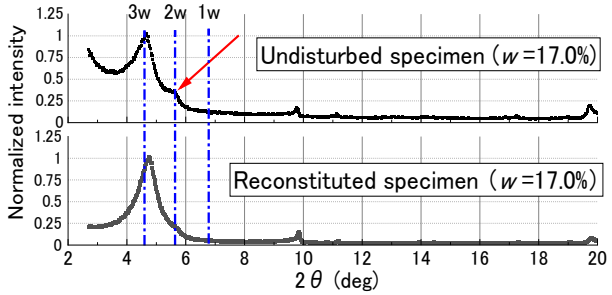

Figure 15. Peak shape comparison between undisturbed and reconstituted specimens (17.0% water content)

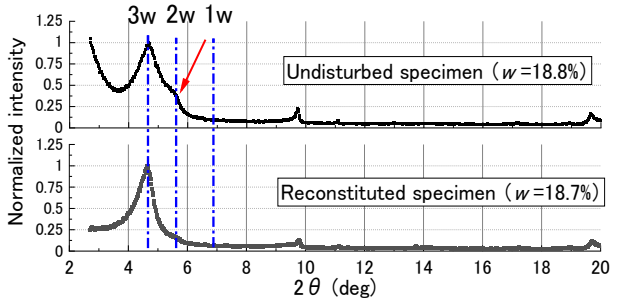

Figure 16. Peak shape comparison between undisturbed and reconstituted specimens (18.8% water content)

5 CONCLUSIONS

This study was conducted for the quantitatively evaluation of the change in swelling characteristics associated with the cementation of bentonite buffer material during geological disposal of HLW. The bentonite ore produced by diagenesis in the natural ground was used for the experimental measurement of swelling pressure and montmorillonite basal spacing as a similar material to the consolidated buffer material. Results obtained from this study indicate the following conclusions.

- Because of the cementation effects, undisturbed specimens have a longer convergence time to reach the maximum swelling pressure. The maximum swelling pressure is about half or less of that of the reconstituted specimens with the same range of dry densities.
- When the montmorillonite basal spacing d_{001} was measured using XRD for the specimens before and after the swelling pressure measurement, the relation between d_{001} and the water contents of the undisturbed specimens and the reconstituted specimens was almost identical when particularly addressing the maximum peak.
- At water contents of 17.0% and 18.8%, the peaks for two rows of water molecules remained in the undisturbed specimens. Therefore, the undisturbed specimens might have fewer water molecules between the montmorillonite crystal layers than the reconstituted specimens. In the undisturbed specimens, the cementation effects inhibited the movement of water molecules between the montmorillonite layers. Consequently, the swelling pressure of undisturbed specimens was reduced to about half.

6 ACKNOWLEDGMENTS

Part of this research was supported by the Ministry of Economy, Trade and Industry (METI) of Japan. Some of the present work was performed as a part of the activities of the Research Institute of Sustainable Future Society, Waseda Research Institute for Science and Engineering, Waseda University. The authors thank Dr. M. Ito of Kunimine Industries, Co. Ltd., for providing bentonite ore samples. All XRD tests were conducted at the Materials Characterization Central Laboratory, Waseda University (Izutani et al. 2016).

7 REFERENCES

Alexander, W.R., Reijonen, H.M., and McKinly, I.G. 2015. Natural analogues: studies of geological processes relevant to radioactive waste disposal in deep geological repositories, *Swiss Journal of Geosciences* 108, 75-100.

Ferrage, E., Lanson, B., Sakharov, B.A., and Drits, V.A. 2005. Investigation of smectite hydration properties by modeling experimental X-ray diffraction patterns: Part I. Montmorillonite hydration properties. *American Mineralogist* 90, 1358-1374.

Ito, H., Suzuki, K., and Komine, H. 2006. Compaction and hydraulic peoperties of granular bentonites and its simplified evaluation method. *Journal of Japan Society of Civil Engineers* 62(4), 803-813 (in Japanese with English abstract)

Ito, M., Ishii, T., Nakashima, H., and Hirata, Y. 1999. The study of genesis and formation condition of bentonite. *Journal of the Clay Science Society of Japan* 38(3), 181-187 (in Japanese)

Izutani, C., Fukagawa, D., Miyashita, M., Ito, M., Sugimura, N., Aoyama, R. et al. 2016. The materials characterization central laboratory: an open-ended laboratory program for fourth-year undergraduate and graduate students. *Journal of Chemical Education* 93(9), 1667-1670.

Japan Atomic Energy Agency (JAEA), Current research and development on geological disposal technology at the Japan Atomic Energy Agency (JAEA), Geological Disposal Research and Development Coordination 1st Meeting (May 31st , 2017), https://www.meti.go.jp/committee/kenkyukai/energy_environment/chisou_shobun_chousei/pdf/001_02_02.pdf, p.29 (2017)

Japanese Geotechnical Society (JGS). 2009. Determination of cation exchange capacity. JGS0261-2009 (in Japanese)

Japanese Industrial Standards (JIS). 2019. Test method for methylene blue adsorption on bentonite and acid clay. JIS Z 2451 (in Japanese)

Komine, H. and Ogata, N. 1991. Evaluation of clay compaction characteristics by means of the plastic limit. *Journal of Japan Society of Civil Engineers* 436(III-16), 103-110 (in Japanese with English abstract)

Komine, H., Yasuhara, K., and Murakami, S. 2009. Swelling characteristics of bentonites in artificial seawater. *Canadian Geotechnical Journal* 46, 177-189.

Morodome, S., and Kawamura, K. 2009. Swelling behavior of Na- and Ca montmorillonite up to 150°C by *in situ* X-ray diffraction experiments. *Clays and Clay Minerals* 57(2), 150-160.

Ogata, N., Kosaki, A., Ueda, H., Asano, H., and Takao, H. 1999. Execution techniques for high level radioactive waste disposal: IV Design and manufacturing procedure of engineered barriers. *Journal of Nuclear Fuel Cycle and Environment* 5(2), 103-121 (in Japanese with English abstract)

Pusch, R. 1983. Stability of deep-siterd smectite minerals in crystalline rock -chemical aspects. *SKBF KBS Teknisk Rapport* 83-16, 1-68.

Sato, T., Watanabe, T., and Otsuka, R. 1992. Effects of layer charge, charge location, and energy charge on expansion properties of dioctahedral smectites. *Clay and Clay Minerals* 40(1), 103−113.

Sawada, T. 1996. Approach for origin elucidation of bentonite bed based on diagenesis. *Newsletter of the Research Community of Smectite* 6(2), 13-22 (in Japanese)

Towhata, I., Kuntiwattanakul, P., Ohishi, K., and Takeuchi, N. 1998. Effect of elevated temperature on mechanical behavior of clays. *Soil Mechanics and Foundation Engineering* 46(10), 27-30 (in Japanese)

Wang, H., Shirakawabe, T., Komine, H., Ito, D., Gotoh, T., Ichikawa, Y., and Chen, Q. 2020. Movement of water in compacted bentonite and its relation with swelling pressure. *Canadian Geotechnical Journal* 57(6), 921-932.

Watanabe, T., and Sato, T. 1988. Expansion characteristics of montmorillonite and saponite under various relative humidity conditions. *Clay Science* 7, 129-138.